Stevens D, Wiebe L. 2019. Experimental testing of a replaceable connection for seismically designed concentrically braced steel frames. *ASCE Journal of Structural Engineering*, 145(4): 04019012, DOI 10.1061/(ASCE)ST.1943-541X.0002283.

Experimental Testing of a Replaceable Connection for Seismically Designed Steel Concentrically Braced Frames

Daniel Stevens, Graduate Student, Department of Civil Engineering, McMaster University, Hamilton, Ontario, Canada

Lydell Wiebe, Assistant Professor, Department of Civil Engineering, McMaster University, Hamilton, Ontario, Canada

Abstract

For a seismically designed concentrically braced frame with hollow structural sections as braces, the typical connection design consists of a slotted brace that is field welded to a gusset plate. During an earthquake, the brace is expected to buckle out-of-plane and the gusset plate is expected to yield. This makes it difficult to repair or replace the brace and connection, and the out-of-plane brace buckling caused by this connection can also damage surrounding walls and cladding, with potential life safety implications. In this paper, an alternative connection is proposed that is expected to result in reduced erection costs by avoiding site welding, and also to simplify structural repairs following a major earthquake by confining all damage to a replaceable brace module. Additionally, the new connection causes the brace to buckle in-plane during a seismic event, reducing the potential for damage to the surrounding walls and cladding. This paper discusses large-scale quasi-static cyclic testing of eight brace modules with two variations of the new connection, one with a single shear eccentric splice and the other with a double sided concentric splice. All of the tested specimens had the desired failure progression and buckled in-plane, as intended. Bolt slip in the connection had very little effect on the overall force-deflection response after the brace compressive strength degraded to less than the slip load. The brace module was replaced after each test without observable damage outside the module. Although

both connection variations behaved in a desirable manner, the single shear eccentric splice was preferred because of the simpler constructability and improved performance.

Introduction

Concentrically braced frames (CBFs) are commonly used as steel lateral force resisting systems throughout North America, including in regions of high seismicity. CBFs have the high strength and stiffness that are necessary for them to be serviceable under wind loads and smaller earthquakes. During severe earthquakes, the energy dissipation to prevent collapse and ensure life safety is provided through tensile yielding and compression buckling of the braces. Hollow structural sections (HSSs) are desirable for braces because their high compressive resistance results in a well-balanced response between paired braces, their ease of transportation and because they suffer less degradation in their compressive strength and energy dissipation than other structural sections (Lee and Bruneau 2005).

Although the brace is the primary member in the design, the brace end connections play an essential role in enabling the brace to perform as intended. North American seismic design specifications require that that the connection must allow the brace end to rotate during buckling, or else the brace must be designed as fully restrained (CSA 2014, AISC 2010). Gusset plate connections with a linear or elliptical clearance rule are normally used to allow brace end rotations (Astaneh-Asl et al. 1985, Lehman et al. 2008). A typical detail for a connection using HSS braces is shown in Fig. 1(a). The brace is slotted and welded directly to the gusset plate requiring field welding that can increase costs and complicate quality control. Furthermore, if the brace and gusset plate are damaged during a major earthquake, replacing them would require cutting out the gusset plate, welding a new plate on site and welding a new brace to the gusset on site. This would likely be an expensive and time consuming process, thus delaying the building's return to safe occupancy.

During a major earthquake, the typical gusset plate connection will cause the brace to buckle out-of-plane. The out-of-plane displacement can be very large, with full-scale testing showing over 400 mm of displacement before brace fracture occurs (Tsai et al. 2013). This out-of-plane deflection can cause damage to exterior cladding and could result in sections falling (Bruneau et al. 2011), endangering the lives of people evacuating the building and of other pedestrians. If the cladding has sufficient strength to restrict the buckling of the brace, the intended behavior of the system would be altered and could invalidate a number of design assumptions, causing the system to fail in a less ductile manner, such as gusset plate buckling due to the unexpectedly high compression force (Sen et al., 2013).

Previous research on bolted connections for CBFs with HSS braces focussed on bolted splice plates to traditional gusset plates (Kotulka 2007, de Oliveira et al. 2008) and connections intersecting braces in single story X-bracing (Davaran et al. 2015). These connections are easier to install than traditional welded connections but may not be easier to replace because damage still occurs in the gusset plates during major earthquakes (de Oliveira et al. 2011). Additionally, previously tested bolted CBF connections exhibited failure in the connection prior to brace buckling or yielding due to multiple plastic hinges forming within the connection, preventing the desired ductile response of the brace (Kotulka 2007, Powell 2010, Davaran et al. 2015). Some research and testing has been done on a knife plate connection that allows brace buckling to occur in-plane (Tsai et al. 2013). This connection, shown in Fig. 1(b), consists of a rotated knife plate connected to a slotted gusset plate. This connection allows in-plane buckling but still requires field welding to install or replace. Recent testing has also shown that the connection may still buckle out-of-plane due to hinging occurring in the gusset plate, negating the intended purpose of the in-plane buckling connection (Sen et al. 2016). To prevent this, Sen et al. (2016) suggest the use of brace shapes with a weak axis that promotes in-plane buckling, although this increases the imbalance between the expected tension and compression forces in the braces.

This paper discusses the design and testing of a new connection that improves the constructability and replaceability of CBFs designed with HSS braces and that causes the brace to buckle in-plane. The new connection was designed to meet three criteria: (1) The new connection should be easy to install and to replace in the event of damage. Specifically, the connection should not require any field welding. If the brace is damaged in an earthquake, the damage should be confined to a module that can be unbolted and replaced as a unit. (2) The new connection should allow the brace to buckle in-plane to minimize damage to surrounding walls and cladding. (3) The new connection should provide comparable performance to current design practice. This includes similar yield and failure progression and similar energy dissipation behavior.

Replaceable Connection Design

As shown in Fig. 2, the new replaceable connection design consists of a hinge plate that is welded to a slotted HSS brace. The hinge plate is bolted to support plates that are welded directly to the beam flange during fabrication. The support plates are sufficiently stiff to confine plastic rotation to the hinge plate so that damage occurs only in components that may be easily replaced. The rotated hinge plate ensures that the brace will buckle in-plane, minimizing damage to the surrounding walls and cladding.

Two variations of this new connection design were developed. The single-shear variation (Type S), shown in Fig. 2(a), uses a single-sided splice connection to attach the hinge plate to the stiffened support plate. This type of connection is very easy to install and replace but introduces eccentricity to the hinge plate. The double-shear variation (Type D), shown in Fig. 2(b), uses a double-sided splice to connect the hinge plate and the support plate. There are three plates used as part of the splice: on one side, the splice plate extends the full width of the hinge plate, while two plates are used on the other side to accommodate the support plate stiffener. Relative to connection Type S, this connection eliminates the hinge plate eccentricity but is more difficult to erect and results in a longer connection for the same brace size. Further information about the conceptual development of these alternatives is provided elsewhere (Stevens and Wiebe, 2016).

In addition to promoting in-plane buckling and improving constructability and replaceability, there are other potential benefits over traditional connections for CBFs because of the lack of a gusset plate connected to the beam and column. The omitted gusset plate means that the new connection is less susceptible to multiple plastic hinges forming within the connection, as has occurred in previous bolted splice tests (Kotulka 2007, Powell 2010, Davaran et al. 2015), and is also less susceptible to an unintended buckling direction that is possible with a knife plate connection (Sen et al. 2016). It also reduces the likelihood of inelastic deformation and damage in the beam and column that can occur due to the forces that develop in the gusset plate at large deformations.

Experimental Program

To verify that the new connection design could satisfy the desired criteria, an experimental program was performed to assess the connection's behavior under quasi-static, cyclic, uniaxial loading. The dimensions of the test represented a 3/4 scale of a reference structure designed to resist the seismic demands in Vancouver, British Columbia. Fig. 3 shows the reference structure and Fig. 4 shows the scaled second story braced bay. The braces in this bay were designed to resist the forces resulting from an equivalent static force procedure of the reference structure following the Canadian code (NBCC-10). All linear dimensions of the design, including brace and plate dimensions, weld thickness and length, and bolt diameter, were scaled by 3/4 and resulted in the design of the base case specimen, S-1, from which the other test specimens varied. For this experiment, the tested region consisted of the brace and the new connection, with angled supports to represent the boundary condition of the beam. Fig. 5 shows a typical experiment setup for the HSS brace specimens that were tested. The angled supports at either end of the brace were designed to behave elastically throughout testing. The triangular section was built from 1” thick plates, a 2” thick plate was used to connect it to the actuator, and the support plate and stiffener that connect to the hinge plate were designed to be the same thickness as the associated hinge plate. Two different angled support details were fabricated, as seen in Fig. 5, and the same supports were reused for all tests of the same connection type.

Load was applied to the specimen using an actuator with a 1060kN capacity that was bolted to one of the angled supports and secured to the strong floor. The loading was applied cyclically and quasi-statically following the ATC-24 testing protocol (ATC 1992). The displacement for each cycle was applied in increments of yield drift (Δ_y), defined as the expected drift at which first buckling occurs. If the brace did not fracture by the end of the protocol shown in Fig. 6, paired cycles at +1 Δ_y relative to the previous displacement were performed until failure. During two of the eight tests, several tension cycle displacements were limited by the force capacity of the actuator.

Test Specimens

Eight cold-formed HSS braces were tested for this experimental program. Most braces were CSA G40.20 Class C members, while two braces were ASTM A500 Grade C. The distance between connection ends was kept constant between all specimens (3768 mm) and the brace lengths were adjusted according to the length of each connection. Five braces were tested with the Single-Shear (Type S) connection and three braces were tested with the Double-Shear (Type D) connection. All specimens were designed to satisfy the requirements for moderately ductile concentrically braced frames in the CSA S16-14 seismic provisions (CSA 2014). The bolted connections of all specimens used ¾” ASTM A325 bolts that were pretensioned to 70% of their expected tensile loading using a torque wrench, but were not designed for a specified slip load. This was done because designing the connections as slip-critical would have required significantly more bolts, resulting in a much longer connection and shorter brace, thereby reducing the energy dissipation capacity of the brace. The weld and bolt bearing strengths in all connections were capacity designed to resist the full overstrength capacity of the braces using the equations given in CSA S16-14 (CSA 2014).

Table 1 summarizes key parameters of the test specimen braces, including the brace shape, brace standard, the connection type, the brace yield (F_y) and ultimate stress (F_u), actual brace lengths, and the predicted tension (T_r) and compression (C_r) resistances of the brace. All wall thicknesses were within 5% of nominal values, including for braces designated as ASTM A500. The brace yield and ultimate stresses were taken from mill certificate values. The predicted tensile resistance, T_r, was calculated as A_gF_y where A_g is the gross area of the brace. The predicted compression resistance, C_r, was calculated using the flexural buckling equation from S16-14 with n being 1.34 for a cold formed HSS and KL being the length between hinge zones (K=1), as recommended in the CISC Commentary of S16-14 and previous research (CSA 2014, Tremblay et al. 2003).

Table 2 summarizes key parameters of the test specimen connections, including the connection length, the hinge and splice plate thicknesses, the hinge length, plastic moment capacities of the brace, hinge plate and splice plates, and a theoretical effective length factor (K_t) based on the relative plastic moment capacities. The hinge plate thickness was designed to provide sufficient tensile resistance along the first line of bolts for the full overstrength capacity of the brace. In addition, the hinge plates of connection Type S were designed to account for the eccentricity present in the connection as recommended by AISC Design Guide 24 for the compressive strength of single sided shear splice connections for HSS members (Packer et al. 2010). In particular, the hinge plate thickness was selected to satisfy the constraint:

$$\frac{P}{P_u} + \left(\frac{8}{9}\right)\left(\frac{M}{M_u}\right) < 1 \quad (1)$$

where P_r is the axial force in the connection caused by the brace compressive force including overstrength, P_c is the factored resistance in axial compression of the thinner splice plate with an effective length of 1.2 times the length of the hinge plate between the brace end and the last line of bolts, M_r is the moment in the connection, which is taken as P_r times half the connection eccentricity, and M_c is the factored plastic flexural capacity of the thinner plate. When designing the test specimens, the resistance factor of P_c and M_c was taken as 1.0. Designing for this constraint resulted in hinge plates that were 14%-24% thicker than if eccentricity had not been considered. The splice plates were designed to provide sufficient tensile resistance along the first line of bolts for the full overstrength capacity of the brace. Half of the tensile force was assumed to be transferred through the large splice plate and the other half was evenly distributed between the two smaller splice plates, causing the small splice plate thickness to be the limiting factor in the design.

The hinge length, defined as the distance between the brace end and the end of the support plate in connection Type S and the end of the splice plate in connection Type D, was typically designed to be two times the hinge plate thickness to align with previous recommendations for gusset plates (Astaneh-Asl et al. 1985). The plastic moment capacity of the brace, M_{pb}, was calculated using the actual yield strength of the braces. The plastic moment capacity of the hinge plate, M_{ph}, was calculated using the specified yield strength of 350MPa. The plastic moment capacity of the splice plates, M_{ps}, was calculated as the tension-compression couple formed when both splice plates reach their specified yield strengths. A theoretical effective length factor, K_t, was also calculated using the relative plastic moment capacities of the brace and hinge plates as seen in Equation 2 (Takeuchi & Matsui 2015):

$$K_t = \frac{1}{1+\left(\frac{M_{ph}}{M_{pb}}\right)} \tag{2}$$

Specimens S-1, S-2 and S-3 were three different brace sizes with the single-shear connection. Specimens D-1, D-2 and D-3 were the same three brace sizes but with the double-shear connection instead. Specimen S-4 was the same as S-1 except that a larger hinge length of three times the hinge plate thickness was used. Specimen S-5 was not designed to account for the eccentricity in the connection and therefore had a hinge plate that was 24% thinner than the hinge plate of S-1.

Experimental Results

The following sections discuss the experimental results in terms of the yield and failure progression, the measured drift and force capacities, and the bolt slip behavior. The load was measured using a load cell connected to the head of the actuator. The axial displacement was measured using a string potentiometer attached to just outside the support plates on either end of the test assemblage, as seen in Fig. 5. These locations correspond to just inside the beam flanges of the reference frame. The axial displacement was converted to an equivalent story drift based on the scaled design building used to select the braces, with a 1% drift corresponding to a 23 mm axial displacement as measured by the potentiometer. Other instrumentation was used to verify the shown data and to record other data, including a string potentiometer to measure the brace axial displacement, string potentiometers along the length of the brace to measure lateral displacement and deflected shape, and an LVDT within the actuator that controlled the applied displacements. All instrumentation was calibrated for use within the testing range.

Yield and Failure Behavior

All eight tested specimens experienced yielding and failure only in the intended locations. The initial yield mechanism was brace buckling, followed by brace tensile yielding and hinge plate flexural yielding. Large compressive deformations caused local cupping to occur near midlength of the brace, which led to low-cycle fatigue failure in the corners of the HSS under tension loading. Eventually, the cracks propagated to cause complete fracture of the brace in tension, as seen in Fig. 7. This is consistent with the failure behavior observed with more conventional gusset plate connections (e.g. Roeder et al. 2011).

For braces with the single-shear connection, the location of hinge plate flexural yielding varied depending on the end of the brace and the direction of buckling. Fig. 8 shows an example of this slightly asymmetrical hinge plate yielding, which was consistent for all specimens with the single-shear connection and occurred because the support was on the opposite side at the top and bottom. The hinge plate at the top rotated towards the support plate, confining yielding to the region between the brace end and the support plate. Yielding in the bottom plate was spread over a larger area, with the most significant yielding occurring along the first row of bolts. Despite hinging occurring along the bolt line of the bottom hinge plate, no tears or unintended damage developed in the hinge plate of any of the single-shear brace specimens, including the thin hinge plate of specimen S-5.

For the double-shear connection, the splice plates were designed to have a higher combined plastic moment capacity than the hinge plate, as shown in Table 2. As intended, the end rotation was confined to the hinge plate for Specimens D-1 and D-2, as shown in Fig. 9(a) and (c). However, in specimen D-3, rotation and yielding appeared first in the two smaller splice plates at one end (bottom of Fig. 9(b)), starting at 1% drift. No yielding was observed in the larger opposing splice plate at this drift level. As the brace end rotation increased, the opposing splice plate (right splice plate in Fig. 9(d)) was engaged, allowing yielding to develop in the hinge plate at 1.6% drift. At larger drifts, the rotation occurred primarily in the hinge plate. Although the overall response of the brace module in compression was still dominated by brace buckling, a similar early yielding in the splice plates at both ends might have led to inelastic deformation concentrating in the connections instead of the brace.

Drift Capacity

Fig. 10 shows the load-displacement curves of the eight specimens tested in the experimental program. All of the tested specimens reached at least the 18^{th} load cycle shown in Fig. 6. The maximum drift ranges, shown in Table 3, varied from 3.3% to 6.4%, which was within the expected range of traditional gusset plate connections (Roeder et al. 2011). The drift range of each test specimen was primarily influenced by the brace shape used. Specimens using the HSS102x102x6.4 section (S-1, S-4, S-5, D-1) all had drift ranges of 3.3% to 3.4%, the smallest among the shapes tested. The HSS 89x89x6.4 specimens S-3 and D-3 had drift ranges of 5.4% and 5.1%, respectively. The variation in drift range between different brace shapes was mostly related to how quickly local cupping occurred in the midlength plastic hinge of the brace, which is heavily influenced by the local slenderness of the brace, as seen in previous experiments (e.g. Han et al. 2007). Using a specified yield strength of 350 MPa, the limit for the width-to-thickness ratio of an HSS is 17.6 in CSA S16-14 (CSA 2014) and 15.3 in AISC 341 (AISC 2010). The HSS102x102x6.4 brace design width-to-thickness ratio of 14.1 only marginally meets these requirements, whereas the values for the other braces shapes (12.0 for HSS89x89x6.4 and 9.0 for HSS89x89x8.0) exceed the requirements by a greater margin.

Very similar drift ranges were found between specimens with the same brace type but different connections (S-1, S-4, S-5 and D-1, S-2 and D-2, S-3 and D-3). Although the HSS 89x89x8 specimens S-2 and D-2 had the largest drift ranges of 5.9% and 6.4% respectively, this may have been influenced by the tension load on these specimens being limited by the actuator capacity, as discussed below.

Force Capacity

The braces and connections of all specimens sustained at least the anticipated tension and compression forces before ultimate failure of the brace. The maximum predicted and measured tension and compression values for each test are shown in Table 3. The maximum tension forces in the experiment, T_{max}, were typically within 10% of the expected yield values, except that specimens S-2 and D-2 were not able to be tested to their full expected yield because the significant material overstrength relative to the nominal yield stress caused them to exceed the actuator capacity.

The maximum recorded compression forces, C_{max}, were 6%-40% larger than the estimated compressive resistance found when using KL equal to the length between hinge zones. An experimentally derived effective length factor, K_e, was calculated by reversing the flexural buckling equation from S16-14 and substituting C_{max} to solve for K (CSA 2014). The experimentally derived effective length factors were all within 12% of the effective length calculated using equation 2 (K_t). This verifies that an effective length estimate that incorporates the relative moment capacities is more accurate than assuming the effective length is the distance between hinge zones (Takeuchi & Matsui 2015). This is especially important for the proposed connection because the hinge plates are typically thicker than a traditional gusset plate for the same brace shape, resulting in greater stiffness in the hinge region.

All specimens with the double-shear connection (D-1, D-2 and D-3) had a lower compression force than the same brace size with the single-shear connection (S-1, S-2 and S-3), despite having a shorter brace length. The reduced compressive strength resulted from the increased connection flexibility caused by the longer connection, even in specimens D-1 and D-2, which had plastic rotation only in the hinge plate (Fig. 9(a)). This difference in connection stiffness is reflected in the effective length factors calculated using equation 2 (K_t in Table 3). Specimen D-3 had a maximum compressive force 18% smaller than S-3 because the early flexural yielding of the pair of splice plates at one end (Fig. 9(b)) greatly increased the flexibility in the connection. As discussed previously, if this had occurred in the splice plates at both ends, brace buckling might not have occurred, with inelastic deformation concentrating in the connection instead.

Specimen S-5, which used a thin hinge plate, had a peak compressive load only slightly smaller than Specimen S-1 and did not have its compressive strength limited by the connection strength. The support plates provided sufficient fixity to the connection to prevent the connection failure modes found in standard lap splice connections in compression (Davaran et al. 2015). This indicates that designing the hinge plate of the single-shear connection to resist the additional moment due to the eccentricity was unnecessarily conservative in this case.

Bolt Slip

Due to the bolted connections of the tested specimens being designed only for strength, bolt slip was observed during the testing of all specimens. Initial bolt slip typically occurred before initial brace buckling and at a load greater than the predicted slip load of the connection (see Table 3), which was calculated using the formula for bolt slip in S16-14 assuming clean mill scale surfaces (CSA 2014). Slip continued in pre-yield cycles but generally in smaller increments and at lower loads than the initial slip, the average load of which is shown in Table 3. However, bolt slip diminished, and eventually stopped, after the brace compressive strength degraded to less than the slip load after the first several post-buckling cycles (Fig. 11(a)). After this, the compressive load no longer exceeded the residual slip load and the connection remained fully slipped in the tensile direction. This meant that slip did not continue to affect the hysteretic response beyond 0.2% to 0.4% drift, as seen in the full specimen hystereses in Fig. 10. Minor damage was present on the bolts, with a visible line apparent at the shear planes. However, no significant bolt deformation was observed. Additionally, despite multiple instances of slip occurring in each direction, the hinge and support plates were sufficiently thick to prevent noticeable deformation of the bolt hole, allowing the support plates to be reused for multiple tests. Bolt slip was larger in specimens with the double-shear connection because there was an additional bolted shear transfer at each brace end. Fig. 11(b) is an example of this larger slip compared to the equivalent single-shear brace in Fig. 11(a). Nevertheless, even with this connection, the bolt slip did not affect the hysteretic response beyond the low drift levels.

Conclusions

A new replaceable connection for the seismic design of concentrically braced frames was proposed, and an experimental program studied the performance of eight different braces with the new connection under quasi-static axial loading. The study focused on the yielding and failure behavior of the brace and hinge plate of the new connection without considering frame effects. The study found that:

1. All braces tested with the new connection failed in the intended manner, with significant yielding occurring at the center and ends of the replaceable brace module before ultimate failure in the brace. The brace performance was primarily influenced by the brace shape rather than connection parameters. Drift ranges were within expected values based on previous studies of more conventional gusset plate connections.
2. Eccentricity in the brace connection did not result in any undesirable yielding or failure. Additionally, designing the hinge plate for extra forces due to eccentricity was unnecessarily conservative in the case that was tested, provided that the support plates had sufficient rotational restraint to prevent multiple plastic hinges from forming in the connection.
3. Bolt slip had little effect on the brace hysteresis after the compressive strength of the brace decayed to less than the slip load. Bolt slip at low displacements was larger in the double-shear connection than in the single-shear connection.

4. Within this experimental program, the performance of the single-shear connection was equal to or better than that of the double-shear connection, with no observed negatives associated with the eccentricity in the connection, less risk of early connection failure and less bolt slip than the double-shear connection. For these reasons and the improved constructability of a single splice connection, the single-shear connection is the recommended choice for further development and experimentation as an alternative connection for concentrically braced frames.

This study focused on specimens designed for a specific scaled brace bay, and the experiments were limited to testing of the brace and connection behavior without considering the interaction with the rest of the braced frame. Future experimental and numerical testing is needed to investigate how including the proposed connection within a frame affects the connection performance, to determine what design considerations are required for the beam and the beam-column connections, and to assess the likelihood of residual drifts or other access issues interfering with replacement of the brace modules.

Acknowledgements

Funding for this project has been provided by the National Sciences and Engineering Research Council (NSERC), Ontario Centres of Excellence (OCE), the Canadian Institute of Steel Construction (CISC) and the Ontario Erectors Association (OEA). Fabrication services and consultation were provided by Walters Inc. The authors gratefully acknowledge this support.

References

American Institute of Steel Construction (AISC). (2010). "Seismic Provisions for Structural Steel Buildings. ANSI/AISC 341-10", Chicago, United States.

Applied Technology Council (ATC). (1992). “Guidelines for cyclic seismic testing of components of steel structures.” ATC 24.

Astaneh-Asl A., Goel S., Hanson R. (1985). “Cyclic out-of-plane buckling of double-angle bracing,” *Journal of Structural Engineering*, 111(5): 1135-1153.

Bruneau M., Uang C-M., and Sabelli R. (2011). *Ductile Design of Steel Structures*, 2^{nd} Edition, McGraw-Hill Companies Inc.

Canadian Standards Association (CSA). (2014). “Limit States Design of Steel Structures.” *CSA Standard S16-14*, Rexdale, Canada.

Davaran A., Gelinas, A., Tremblay, R. (2015). “Inelastic Buckling Analysis of Steel X-Bracing with Bolted Single Shear Lap Connections.” *Journal of Structural Engineering*, 141(8): 04014204.

de Oliveira C., Packer J., Christopolous C. (2008). “Cast Steel Connectors for Circular Hollow Section Braces under Inelastic Cyclic Loading.” *Journal of Structural Engineering*, 34:3(374): 374-383.

de Oliveira C., Christopolous C., Packer J. (2011). “High-Strength Brace Connectors for use in SCBF and OCBF.” *80^{th} Annual Structural Engineers Association of California Convention*. Las Vegas, Nevada.

Han S. W., Kim W. T., Foutch D. A. (2007). “Seismic behavior of HSS bracing members according to width-thickness ratio under symmetric cyclic loading.” *Journal of Structural Engineering*; 133(2), ASCE.

Kotulka B. A. (2007). “Analysis for a Design Guide on Gusset Plates used in Special Concentrically Braced Frames.” MASc thesis, University of Washington, Seattle, WA.

Lee K., Bruneau M. (2005). “Energy dissipation demand of compression members in concentrically braced frames” *Steel and Composite Structures*, 4(5): 235-358.

Lehman D., Roeder C., Herman D., Johnson S. and Kotulka B. (2008). Improved Seismic Performance of Gusset Plate Connections. Journal of Structural Engineering, 134: 890-901.

Packer J., Sherman D., Lecce M. (2010). “Steel Design Guide 24: Hollow Structural Section Connections.” American Institute of Steel Construction, Chicago, IL, US.

Powell J. A. (2010). “Evaluation of Special Concentrically Braced Frames for Improved Seismic Performance and Constructability.” MASc thesis, Univsersity of Washington, Seattle, WA.

Roeder C. W., Lumpkin E. J., Lehman D. E. (2011). "A balanced design procedure for special concentrically braced frame connections." *Journal of Constructional Steel Research*, 67: 1760-1772.

Sen A. D., Sloat D., Pan L., Roeder C. W., Lehman D. E., Berman J. W. (2013). "Evaluation of the seismic performance of two-story concentrically braced frames with weak beams." *5th International Conference on Advances in Experimental Structural Engineering*, NCREE, Taipei, Taiwan.

Sen A. D., Roeder C. W., Berman J. W., Lehman D. E., Li C. H., Wu A. C., Tsai K. C. (2016). "Experimental Investigation of Chevron Concentrically Braced Frames with Yielding Beams." *Journal of Structural Engineering*, 142(12): 04016123.

Stevens D., Wiebe L. (2016). "Development of a novel replaceable connection for seismically designed steel concentrically braced frames." *5th International Structural Speciality Conference*, CSCE 2016, London, Canada.

Takeuchi T., Matsui R. (2015). "Cumulative Deformation Capacity of Steel Braces under Various Cyclic Loading Histories." *Journal of Structural Engineering*, 141(7): 04014175.

Tremblay R., Archambault M., Filiatrault A. (2003). "Seismic response of concentrically braced steel frames made with rectangular hollow bracing members." *Journal of Structural Engineering*, 129(12): 1626-1636.

Tsai C. Y., Tsai K. C., Lin P. C., Ao W. H., Roeder C. W., Mahin S. A., Lin C. H., Yu Y. J., Wang K. J., Wu C., Chen, J. C., Lin T. H. (2013). "Seismic design and hybrid tests of a full-scale three-story concentrically braced frame using in-plane buckling braces." *Earthquake Spectra*, 29 (3): 1043-1067.

Fig. 1: CBF connections: (a) Typical connection; (b) Knife plate connection

Fig. 2: Replaceable CBF connection variations: (a) Single-Shear (Type S) (b) Double-Shear (Type D)

Fig. 3: Reference Structure in Vancouver, BC

Fig. 4: Scaled frame dimensions for selecting brace size

Fig. 5: Typical Experimental Setup

Fig. 6: Loading Protocol

Fig. 7: Specimen S-1: (a) Local cupping; (b) Tearing; (c) Fracture

Fig. 8: Single-Shear hinge yield lines: (a) Buckled shape; (b) Top hinge; (c) Bottom hinge

Fig 9: Double-Shear hinge behavior: (a) Single hinge line (D-1); (b) Multiple hinge lines (D-3); (c) Profile single hinge (D-1); (d) Profile multiple hinges (D-3)

Fig. 10: Experimental load-displacement curves for all specimens

Fig. 11: Bolt slip comparison: (a) Single-Shear connection S-1; (b) Double-Shear connection D-1

Table 1: Test Brace Details

Specimen	HSS Square Brace Shape	Brace Standard	Connection Type	F_y (MPa)	F_u (MPa)	Brace Length (mm)	Predicted Tension, Tr (kN)	Predicted Compression, Cr, K=1 (kN)
S-1	102x102x6.4	G40.20	Single-Shear	444	501	3082	1030	-494
S-2	89x89x8.0	A500	Single-Shear	513	578	3096	1236	-420
S-3	89x89x6.4	G40.20	Single-Shear	458	531	3200	911	-337
S-4	102x102x6.4	G40.20	Single-Shear	444	501	3034	1030	-501
S-5	102x102x6.4	G40.20	Single-Shear	444	501	3108	1030	-490
D-1	102x102x6.4	G40.20	Double-Shear	444	501	2863	1030	-540
D-2	89x89x8.0	A500	Double-Shear	513	578	2886	1236	-467
D-3	89x89x6.4	G40.20	Double-Shear	458	531	3105	911	-349

Table 2: Test Connection Details

Specimen	Connection Length (mm)	Plate Thickness (mm)		Hinge Length (mm)	Plastic Moment Capacity (kNm)			Theoretical Effective Length Factor, K_t
		Hinge	Splice		Brace, M_{pb}	Hinge, M_{ph}	Splice, M_{ps}	
S-1	686	25	-	50	36.1	10.9	-	0.77
S-2	672	22	-	44	36.6	8.5	-	0.81
S-3	568	19	-	38	27.7	6.3	-	0.81
S-4	734	25	-	75	36.1	10.9	-	0.77
S-5	660	19	-	38	36.1	6.3	-	0.85
D-1	905	19	16	44	36.1	6.3	36.7	0.85
D-2	882	19	16	38	36.6	6.3	36.7	0.85
D-3	663	16	10	32	27.7	4.5	17.0	0.86

Table 3: Summary of Test Results

	Drift (%)			Peak Tension Forces (kN)		Peak Compression Forces (kN)				Slip Loads (kN)	
Specimen	Min	Max	Range	T_r	T_{max}	C_r (K=1)	C_{max}	K_t	K_e	Predicted	Actual[a]
S-1	-1.8	+1.6	3.4	1030	1047	-494	-605	0.77	0.84	374	370
S-2	-3.1	+2.8	5.9	1236	1091[b]	-420	-592	0.81	0.78	374	375
S-3	-2.7	+2.4	5.1	911	1000	-337	-451	0.81	0.80	299	285
S-4	-1.9	+1.5	3.4	1030	1052	-501	-590	0.77	0.86	374	445
S-5	-1.8	+1.5	3.3	1030	1031	-490	-569	0.85	0.88	374	360
D-1	-1.9	+1.4	3.3	1030	1011	-540	-572	0.85	0.94	449	340
D-2	-3.4	+3.0	6.4	1236	1067[b]	-467	-568	0.85	0.87	449	555
D-3	-2.7	+2.2	4.9	911	975	-349	-371	0.86	0.95	299	260

[a]Average of slip loads after initial slip
[b]Limited by actuator

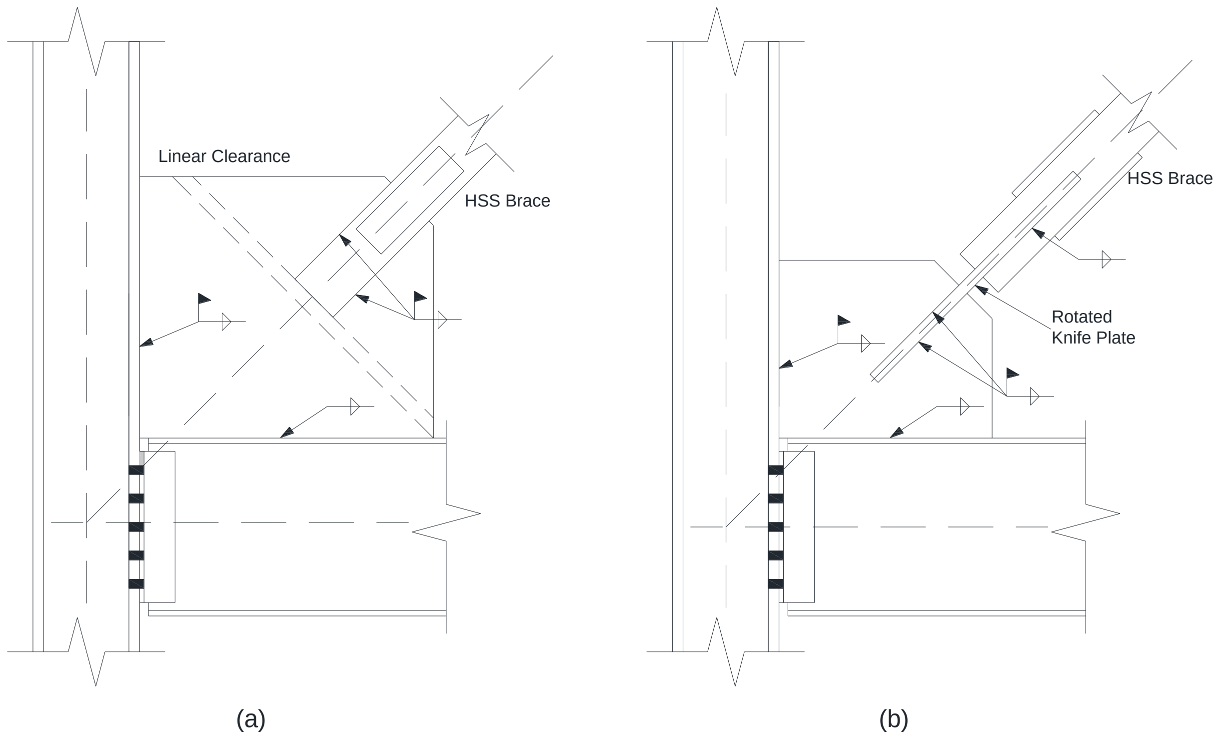

Fig. 1: Concentrically braced frame connections: (a) Typical connection; (b) Knife plate connection

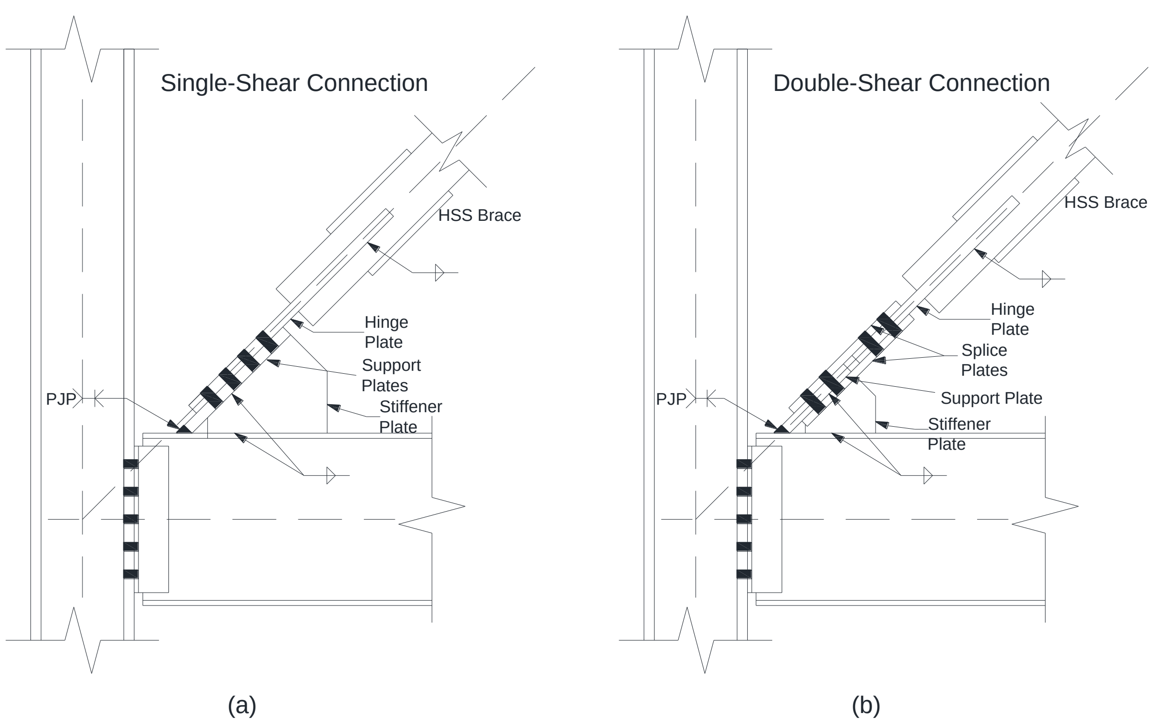

Fig. 2: Replaceable concentrically braced frame connection variations: (a) Single-Shear (Type S) (b) Double-Shear (Type D)

Fig. 3: Reference Structure in Vancouver, BC

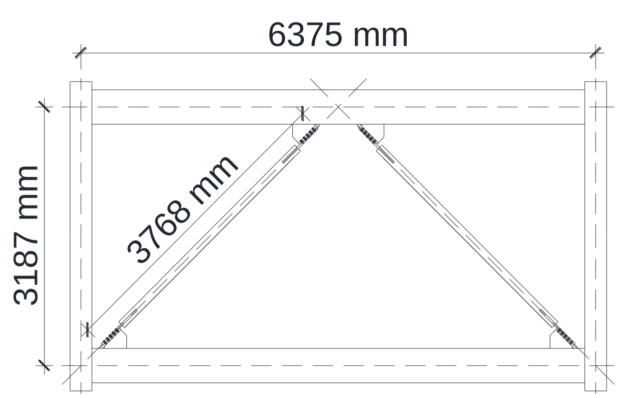

Fig. 4: Scaled frame dimensions for selecting brace size

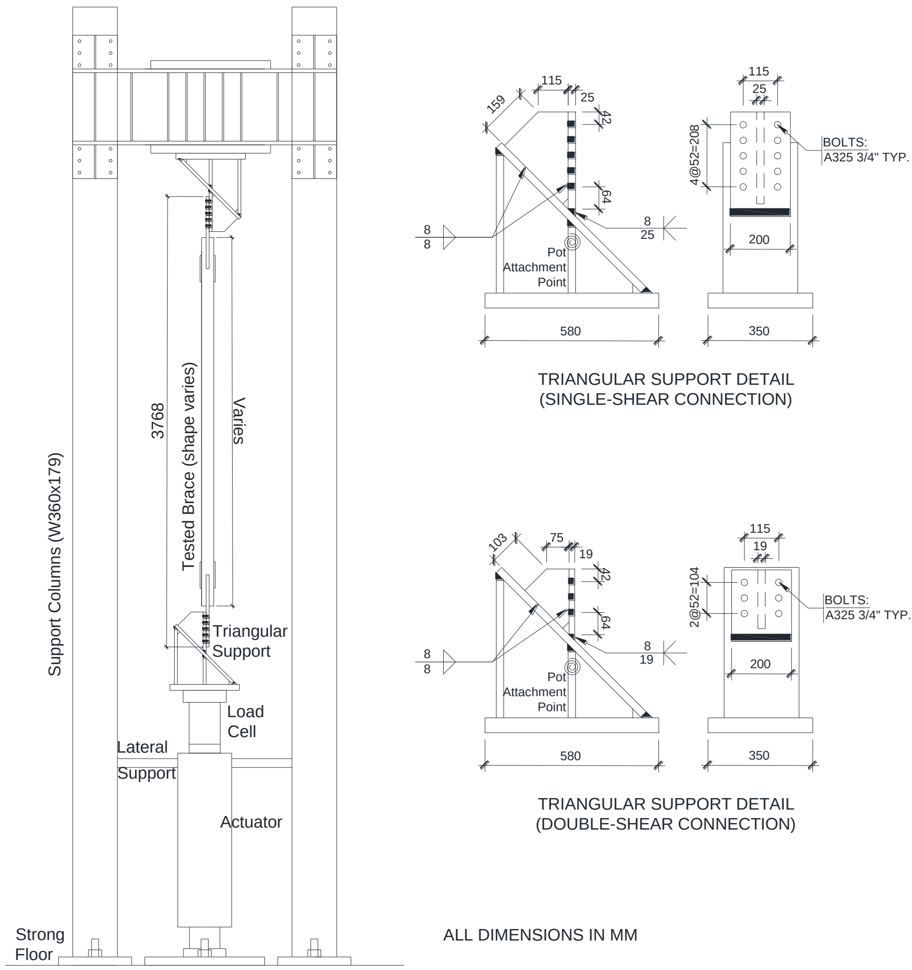

Fig. 5: Typical Experimental Setup

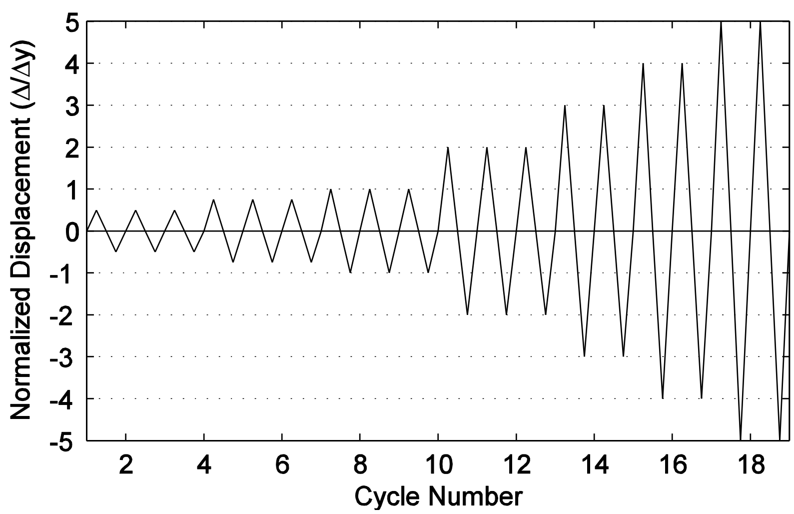

Fig. 6: Loading Protocol

(a) (b) (c)

Fig. 7: Specimen S-1: (a) Local cupping; (b) Tearing; (c) Fracture

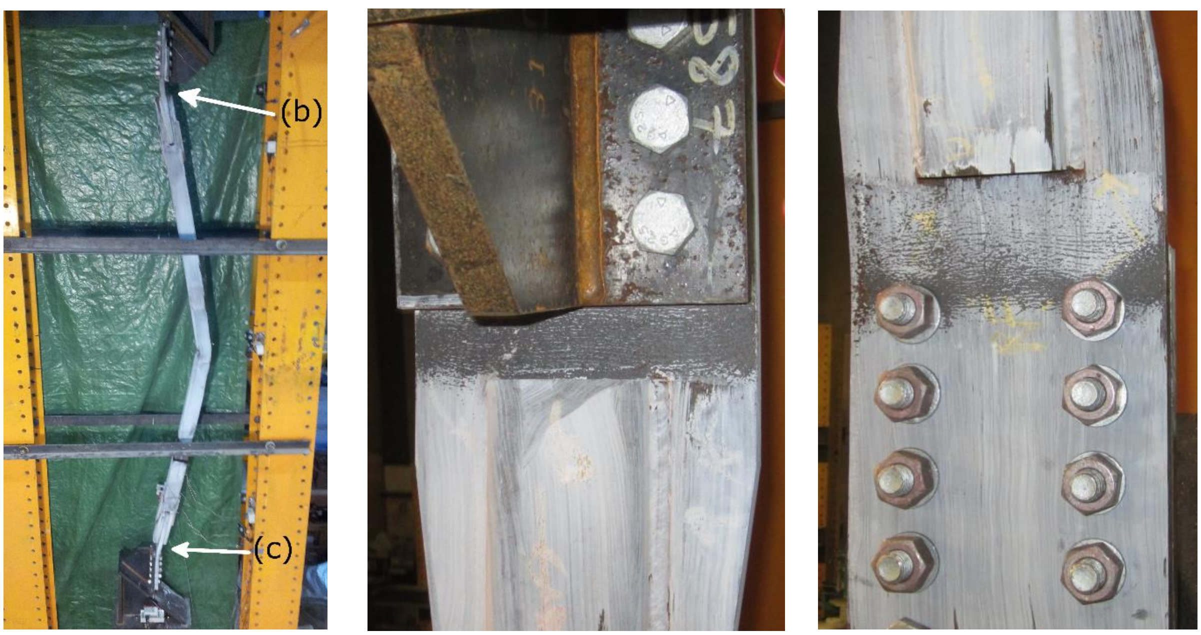

(a) (b) (c)

Fig. 8: Single-Shear hinge yield lines: (a) Buckled shape; (b) Top hinge; (c) Bottom hinge

(a)

(b)

(c)

(d)

Fig 9: Double-Shear hinge behavior: (a) Single hinge line (D-1); (b) Multiple hinge lines (D-3); (c) Profile with single hinge (D-1); (d) Profile with multiple hinges (D-3)

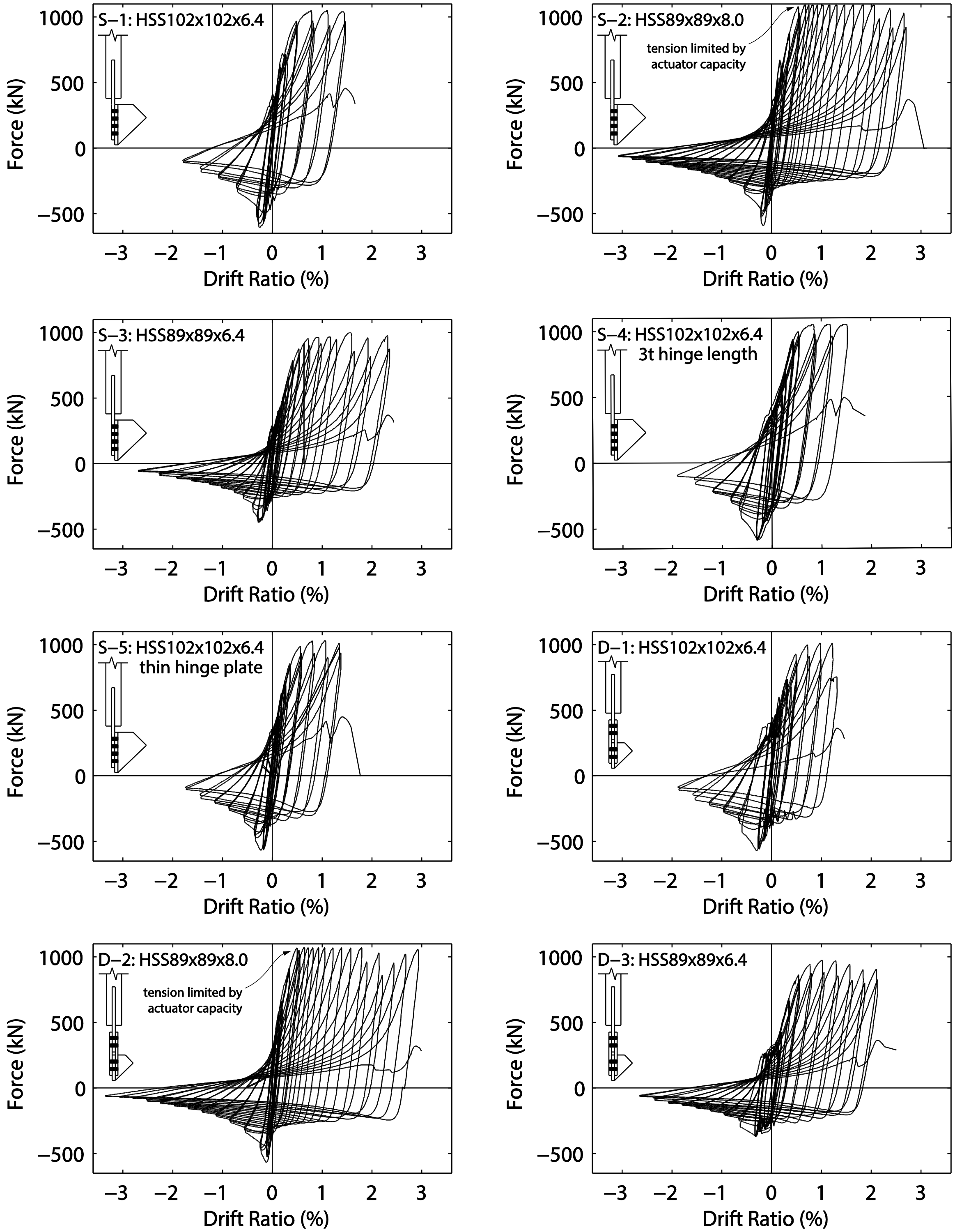

Fig. 10: Experimental load-displacement curves for all specimens

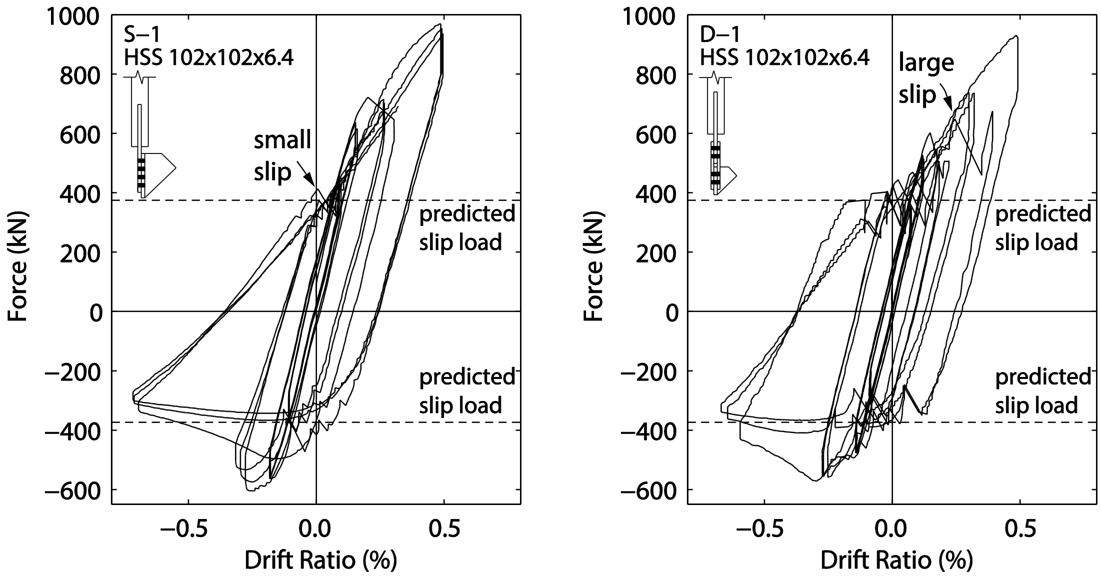

(a) (b)

Fig. 11: Bolt slip comparison: (a) Single-Shear connection S-1; (b) Double-Shear connection D-1